research papers

Structure refinement of the silicon carbide polytypes 4*H* and 6*H*: unambiguous determination of the refinement parameters

A. Bauer,^{a}* Ph. Reischauer,^{a} J. Kräusslich,^{a} N. Schell,^{b} W. Matz^{b} and K. Goetz^{a}

^{a}Institute of Optics and Quantum Electronics, Friedrich Schiller University of Jena, Max-Wien-Platz 1, D-07743 Jena, Germany, and ^{b}Forschungszentrum Rossendorf, Postfach 510119, D-01314 Dresden, Germany. Correspondence e-mail: bauer@esrf.fr

The atomic positions of the silicon carbide (SiC) polytypes 6*H* and 4*H* differ slightly from an ideal tetrahedron. These small deviations can be investigated by X-ray diffraction of so-called 'quasiforbidden' reflections, which are very sensitive with respect to the extremely small variations in the structure. Nevertheless, an unambiguous calculation of the refinement parameters from the absolute values of the structure factors of the 'quasiforbidden' reflections is not possible. In the case of SiC-4*H*, there are two and, in the case of SiC-6*H*, six different structure models, which yield the same absolute values of the structure factors. In order to distinguish between these models, additional phase information about the measured reflections is needed. To achieve this, Renninger-scan (ψ-scan) profiles in the vicinity of three-beam cases are used. These experimentally measured ψ-scans are compared with theoretical calculated profiles for each model. Another method to distinguish the different models is to compare the bond lengths between atoms of the two polytypes, which have equivalent vicinities. For both SiC-4*H* and SiC-6*H*, an unambiguous determination of the structure refinement parameters was possible.

1. Introduction

Silicon carbide (SiC) is a semiconductor (Harris, 1995) that appears in many polytypes (Verma & Krishna, 1966). More than 100 polytypes are known. The most common polytypes are 4*H* and 6*H*. Both polytypes belong to the hexagonal crystal system and the atomic positions obey operations of the space group $P6_3mc$ (C_{6v}^4). The carbon atoms are tetrahedral surrounded by silicon atoms and *vice versa*. Owing to the space group, the positions of the atoms perpendicular to the *c* axis [0001] are fixed, however, they are allowed to move freely parallel to the *c* axis. The bond tetrahedron can be compressed or stretched. The crystal structures of the two polytypes 4*H* and 6*H* are shown in Fig. 1. The characteristic zigzag chains are plotted in the (11$\bar{2}$0) plane. Half of the atoms are labeled $X(1)$ to $X(n/2)$ [$X =$ Si, C, *n* is the number of Si—C bilayers in each polytype (SiC-4*H* $n = 4$; SiC-6*H* $n = 6$)], the other half by $X(1')$ to $X(n'/2)$. The atoms $X(j)$ and $X(j')$ are on equivalent positions in the silicon carbide unit cell ($j = 1, 2, \ldots, n/2$), since according to the space group there is an equivalence of the lower and upper halves of the unit cell. The relative displacements from the ideal tetrahedral positions are $\delta_{nH}(j)$ for the silicon atoms and $\varepsilon_{nH}(j)$ for the carbon atoms. Also according to the space-group symmetry, $\delta_{nH}(j) = \delta_{nH}(j')$ and $\varepsilon_{nH}(j) = \varepsilon_{nH}(j')$. The coordinates of the *n* atoms in the unit cell of these polytypes are, according to

the hexagonal crystal system for SiC-4*H*, for the lower half of the unit cell:

$$(0, 0, \xi(X)), \quad (\tfrac{1}{3}, \tfrac{2}{3}, \tau(X))$$

and, for the upper half:

$$(\tfrac{2}{3}, \tfrac{1}{3}, \tfrac{1}{2} + \xi(X)), \quad (\tfrac{1}{3}, \tfrac{2}{3}, \tfrac{1}{2} + \tau(X));$$

with

$$\xi(\text{Si}) = 0 + \delta_{4H}(1), \quad \xi(\text{C}) = \tfrac{3}{16} + \varepsilon_{4H}(1)$$
$$\tau(\text{Si}) = \tfrac{4}{16} + \delta_{4H}(2), \quad \tau(\text{C}) = \tfrac{7}{16} + \varepsilon_{4H}(2).$$

For SiC-6*H*, the atomic positions are, for the lower half of the unit cell:

$$(0, 0, \xi(X)), \quad (\tfrac{1}{3}, \tfrac{2}{3}, \tau(X)), \quad (\tfrac{2}{3}, \tfrac{1}{3}, \nu(X))$$

and, for the upper half:

$$(0, 0, \xi(X)), \quad (\tfrac{2}{3}, \tfrac{1}{3}, \tfrac{1}{2} + \tau(X)), \quad (\tfrac{1}{3}, \tfrac{2}{3}, \tfrac{1}{2} + \nu(X));$$

with

$$\xi(\text{Si}) = 0 + \delta_{6H}(1), \quad \xi(\text{C}) = \tfrac{3}{24} + \varepsilon_{6H}(1)$$
$$\tau(\text{Si}) = \tfrac{4}{24} + \delta_{6H}(2), \quad \tau(\text{C}) = \tfrac{7}{24} + \varepsilon_{6H}(2)$$
$$\nu(\text{Si}) = \tfrac{8}{24} + \delta_{6H}(3), \quad \nu(\text{C}) = \tfrac{11}{24} + \varepsilon_{6H}(3).$$

Furthermore, there are two possible polarities of the crystal, where in the case of bulk truncation with intact Si—C bilayers the (0001) surface would be silicon terminated, while the (0001) surface would be carbon terminated (Starke, 1997). In this work, the [0001] direction was chosen as the c axis. In the illustration of the unit cells of silicon carbide polytypes (Fig. 1), the the polar 6_3 axis coincides with the c axis for the polytype $6H$, while for the polytype $4H$ the c axis is shifted by a vector $(-\frac{1}{3}, -\frac{2}{3}, 0)$ with respect to the 6_3 axis.

The method we used to obtain the structure-refinement parameters is the investigation of 'quasiforbidden' reflections of the type $h - k = 3r$, l even and $l \neq ns$, where h, k, l are the Miller indices and r, s are integers, $n = 4$ (SiC-$4H$) or 6 (SiC-$6H$) (Bauer et al., 1998, 1999). The structure factor of 'quasiforbidden' reflections $F_{qf}(hkil)$ would be zero if the silicon and the carbon atoms were in the ideal tetrahedral positions. The main advantage of using 'quasiforbidden' reflections for structure refinement is that they are extremely sensitive to small structure variations. Furthermore, a correction for extinction is not needed, since the extinction length is much larger than the absorption length, i.e. $|F_{qf}| \ll |F_0''| = \mu_{SiC} V/(2\lambda r_e)$, where μ_{SiC} is the linear absorption coefficient for SiC, λ the wavelength, V the volume of the unit cell and r_e the classical electron radius ($r_e = 2.818 \times 10^{-15}$ m). Since the atomic displacements $\delta_{nH}(j)$ and $\varepsilon_{nH}(j)$ are very small, approximately of the order of 10^{-4} times the c lattice constant, it is possible to expand the structure factor to the first order of the atomic displacements $\delta_{nH}(j)$ and $\varepsilon_{nH}(j)$. Therefore, we obtain the structure factor

$$
\begin{aligned}
F_{qf}(hkil) = {} & 2f_{Si} \sum_{j=1}^{n/2} 2\pi i l \delta_{nH}(j) \exp[2\pi i l(j-1)/n] \\
& + 2f_C \sum_{j=1}^{n/2} 2\pi i l \varepsilon_{nH}(j) \exp(2\pi i l 3/4n) \\
& \times \exp[2\pi i l(j-1)/n],
\end{aligned} \tag{1}
$$

where f_{Si}, f_C are the atomic scattering factors for silicon and carbon, respectively, and n is the number of Si–C bilayers in each polytype. This structure factor is, for SiC-$4H$:

$$
\begin{aligned}
F_{qf}(hkil) = {} & 2f_{Si} 2\pi i l [\delta_{4H}(1) - \delta_{4H}(2)] \\
& + 2f_C 2\pi i l [\varepsilon_{4H}(1) - \varepsilon_{4H}(2)] \exp(\tfrac{3}{8}\pi i l);
\end{aligned} \tag{2}
$$

and, for SiC-$6H$:

$$
\begin{aligned}
& F_{qf}(hkil) \\
& = 2\pi l f_{Si} \big(\pm 3^{1/2}[\delta_{6H}(2) - \delta_{6H}(3)] - i\{[\delta_{6H}(2) - \delta_{6H}(1)] \\
& \quad + [\delta_{6H}(3) - \delta_{6H}(1)]\} \big) + 2\pi l f_C \big(\pm 3^{1/2}[\varepsilon_{6H}(2) - \varepsilon_{6H}(3)] \\
& \quad - i\{[\varepsilon_{6H}(2) - \varepsilon_{6H}(1)] + [\varepsilon_{6H}(3) - \varepsilon_{6H}(1)]\} \big) \exp(\tfrac{1}{4}\pi i l).
\end{aligned} \tag{3}
$$

Since the expanded structure factor $F_{qf}(hkil)$ contains the parameters $\delta_{nH}(j)$ and $\varepsilon_{nH}(j)$ in linear combinations, only a determination of these linear combinations of the atomic displacements is possible by using exclusively 'quasiforbidden' reflections. Thus we discuss the following two subjects:

(i) Relative changes of the bilayer thickness (Fig. 2):

$$
\begin{aligned}
\frac{\Delta d_{4H}(j)}{d_0} & = \frac{d_{4H}(j) - c_{4H}/4}{c_{4H}/4} \\
& = 4[\delta_{4H}(j+1) - \delta_{4H}(j)] \qquad (\text{SiC-}4H) \tag{4} \\
\frac{\Delta d_{6H}(j)}{d_0} & = \frac{d_{6H}(j) - c_{6H}/6}{c_{6H}/6} \\
& = 6[\delta_{6H}(j+1) - \delta_{6H}(j)] \qquad (\text{SiC-}6H). \tag{5}
\end{aligned}
$$

(ii) Changes of the Si—C bond length in the c direction (Fig. 2):

$$
\begin{aligned}
\frac{\Delta L_{4H}(i;j)}{L_0} & = \frac{L_{4H}(i) - L_{4H}(j)}{3c_{4H}/16} \\
& = \tfrac{16}{3}\{[\varepsilon_{4H}(i) - \varepsilon_{4H}(j)] - [\delta_{4H}(i) - \delta_{4H}(j)]\} \\
& \hspace{5em} (\text{SiC-}4H) \tag{6} \\
\frac{\Delta L_{6H}(i;j)}{L_0} & = \frac{L_{6H}(i) - L_{6H}(j)}{c_{6H}/8} \\
& = 8\{[\varepsilon_{6H}(i) - \varepsilon_{6H}(j)] - [\delta_{6H}(i) - \delta_{6H}(j)]\} \\
& \hspace{5em} (\text{SiC-}6H), \tag{7}
\end{aligned}
$$

where for SiC-$4H$ $i, j = 1, 2$ and for SiC-$6H$ $i, j = 1, 2, 3$. c_{4H} and c_{6H} are the c lattice constants for SiC-$4H$ and for SiC-$6H$, respectively, d_0 is the average distance between two adjacent Si atoms in the c direction and L_0 is the Si—C bond length for the ideal tetrahedron.

Remark 1. All indices in brackets in this paper cannot be larger than $n/2$, e.g., if $j = n/2$, $j + 1$ will be replaced by 1 etc.

2. Ambiguities of the refinement parameters

Since the relaxation parameters were obtained from the absolute values of the structure factor of the 'quasiforbidden' reflections $|F_{qf}(hkil)|$, an unambiguous determination is not possible. This is obvious if we describe the deviations $\delta_{nH}(j)$ and $\varepsilon_{nH}(j)$ of the silicon and carbon atoms from the ideal tetrahedron structure as follows:

$$
\begin{aligned}
\delta_{nH}(j) &= q u_{nH}(j + p - 1) = q u_{nH}(m) \tag{8} \\
\varepsilon_{nH}(j) &= q v_{nH}(j + p - 1) = q v_{nH}(m), \tag{9}
\end{aligned}
$$

where q is -1 or $+1$ and p, m are integers from 1 to $n/2$.

With these parameters, we obtain for the structure factor of (1):

$$
\begin{aligned}
F_{qf}(hkil) = {} & q \exp[-2\pi i l(p-1)/n] \Big\{ 2f_{Si} \sum_{m=1}^{n/2} 2\pi i l u_{nH}(m) \\
& \times \exp[2\pi i l(m-1)/n] + 2f_C \sum_{m=1}^{n/2} 2\pi i l v_{nH}(m) \\
& \times \exp[2\pi i(3/4n)l] \exp[2\pi i l(m-1)/n] \Big\}. \tag{10}
\end{aligned}
$$

Because the two sums in (10) are independent of the variables p and q, one can see clearly that the absolute value of the

research papers

structure factor $|F_{qf}(hkil)|$ does not depend on these variables but the phase of the structure factor $F_{qf}(hkil)$.

This leads to the following consequences:

(i) A determination of the linear combinations of the refinement parameters of (2) and (3) is possible, except for the sign. Therefore, we obtain two models for each polytype. In the following, we will denote these two models with the variable q, whereby q is $+1$ for the positive sign and -1 for the negative sign.

(ii) A simultaneous cyclic permutation of the relaxation parameters $u_{nH}(m)$ and $v_{nH}(m)$ in (10) leads to the same value for the square of the absolute value of the structure factor $|F_{qf}(hkil)|^2$. This means that the relaxation parameters of the one bilayer is assigned to the next bilayer. Owing to the permutations, we obtain two permutation models for the

polytype $4H$ and three for $6H$. These models will be denoted by the variable p. In the case of SiC-$4H$, the value of p is 1 or 2, in the case of SiC-$6H$, $p = 1, 2, 3$.

Overall, there are four models for SiC-$4H$ and six models for SiC-$6H$, with cyclic permutations and for each of these permutation models a positive and a negative variant. We will denote these models by the product $(pq)_{nH}$, where the index n indicates the polytype ($n = 4$ or 6). Thus, the four SiC-$4H$ models are $+1_{4H}$, -1_{4H}, $+2_{4H}$, -2_{4H} and the six SiC-$6H$ models are $+1_{6H}$, -1_{6H}, $+2_{6H}$, -2_{6H}, $+3_{6H}$, -3_{6H}. In the case of SiC-$4H$, we can restrict ourselves to the discussion of the models $+1_{4H}$ and -1_{4H} because a permutation of the relaxation parameters yields the same result as changing the sign.

The refinement parameters [equations (4)–(7)] according to Bauer *et al.* (1999) of our different models are shown in Table 1. In the following, we relate our investigations to these refinement parameters.

Below we present two possibilities to resolve the ambiguities in respect of the structure models of the two SiC polytypes $4H$ and $6H$. One method is based on a comparison of the cell internal structure and the precisely measured c lattice constant of the two polytypes. The other method uses a qualitative comparison of measured and calculated ψ-scan profiles close to three-beam nodes.
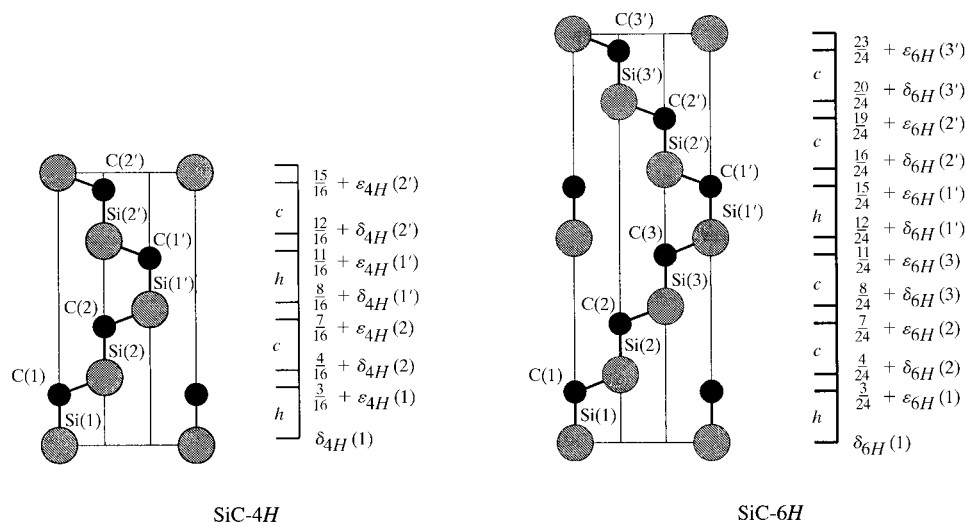

Figure 1
Atomic structures of the SiC polytypes $4H$ and $6H$ [cut through the $(11\bar{2}0)$ plane]. $\delta_{nH}(j)$ and $\varepsilon_{nH}(j)$ are the relative deviations of the Si and C atoms. h denotes the hexagonal Si–C bilayers, c the cubic ones.
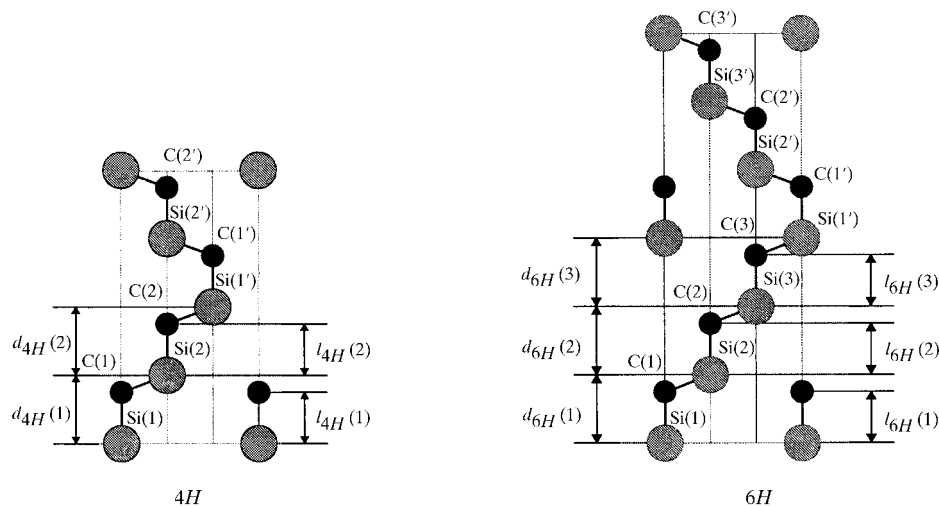
3. Comparison of the cell internal structure of the polytypes SiC-6H and SiC-4H

One possibility to distinguish the six different models of SiC-$6H$ and the two models of SiC-$4H$, respectively, is to compare the internal structure of the two unit cells. This means that the bond lengths and angles in equivalent vicinities of the polytypes $4H$ and $6H$ are comparable. Under this condition, the SiC-$6H$ segment between the silicon atoms Si(3) and Si(2$'$) is comparable with the SiC-$4H$ segment between the atoms Si(2) and Si(2$'$) (Fig. 1). So the SiC-$6H$ crystal structure can be composed of the SiC-$4H$ segment between Si(2) and Si(2$'$) and the SiC-$6H$ segment between Si(2$'$) and Si(3$'$) and an analogous repetition. A comparison of the calculated c lattice constant of such an SiC-$6H$ unit cell with the experimental lattice

Figure 2
Thickness of the Si–C bilayer $d_{nH}(j)$ and bond length in the c direction $L_{nH}(j)$ of the SiC polytypes $6H$ and $4H$.

Table 1
Changes of the thickness of SiC bilayers and Si—C bond length in the c direction in % (Bauer *et al.*, 1999).

p and q denote the permutation and the changing of the sign, respectively. SiC-4H: $p = 1, 2$; SiC-6H: $p = 1, 2, 3$. $q = \pm1$ for both polytypes.

Polytype		%		%
SiC-4H	$[\Delta d_{4H}(p)/d_0]q$	+0.07	$[\Delta L_{4H}(p; p+1)/L_0]q$	+0.18
	$[\Delta d_{4H}(p+1)/d_0]q$	−0.07	$[\Delta L_{4H}(p+1; p)/L_0]q$	−0.18
SiC-6H	$[\Delta d_{6H}(p)/d_0]q$	+0.048	$[\Delta L_{6H}(p; p+1)/L_0]q$	+0.32
	$[\Delta d_{6H}(p+1)/d_0]q$	−0.102	$[\Delta L_{6H}(p; p+2)/L_0]q$	+0.32
	$[\Delta d_{6H}(p+2)/d_0]q$	+0.054	$[\Delta L_{6H}(p+1; p+2)/L_0]q$	0.00

Table 2
Experimental c and a lattice constants of the SiC polytypes 4H and 6H (Bauer *et al.*, 1998).

Polytype	c lattice constant (Å)	a lattice constant (Å)
SiC-4H	10.08480 ± 0.00004	3.08051 ± 0.00006
SiC-6H	15.11976 ± 0.00006	3.08129 ± 0.00004

constant, which was determined by high-precision X-ray measurements (Bauer *et al.*, 1998), allows a distinction of the different refinement models if one uses the following assumption: In the case of SiC-6H, the difference in the Si—C bond length between the two adjacent cubic bilayers [$L_{6H}(2)$, $L_{6H}(3)$] in the elementary cell is negligibly small in comparison to the difference in the Si—C bond length between a hexagonal [$L_{6H}(1)$] and a cubic bilayer. Thus the models obtained by cyclic permutations can be eliminated and we obtain for the relaxation parameters according to Fig. 2 approximately:

$$|\Delta L_{6H}(2; 3)| \ll |\Delta L_{6H}(1; 2)| \quad |\Delta L_{6H}(2; 3)| \ll |\Delta L_{6H}(1; 3)|, \tag{11}$$

respectively. If we permute simultaneously both relaxation parameters $u_{6H}(j)$ and $v_{6H}(j)$ $(j = 1, 2, 3)$ cyclically, this equation would only be satisfied for the models $+1_{6H}$ and -1_{6H}. The other four models ($\pm2_{6H}$, $\pm3_{6H}$) result in an equality of the Si—C bond length of the hexagonal and one cubic bilayer contrary to our assumption. This assumption is also in accordance with theoretical *ab initio* calculations from Käckell *et al.* (1994) and Cheng *et al.* (1990).

According to our model in which the SiC-6H structure is composed of SiC-4H segments and additional cubic bilayers, the c lattice constant of the polytype SiC-6H can be calculated from the SiC-4H c lattice constant and the thickness of the two additional Si–C bilayers. The thickness of these additional bilayers is equivalent to the distance between the silicon atoms Si(2′) and Si(3′) and Si(2) and Si(3), respectively. Only this distance contains the transfer from one cubic bilayer to another cubic bilayer, which does not occur in the SiC-4H unit cell. The value of this bilayer thickness is given by $d_{6H}(2)$ (Fig. 2). For the c lattice constant of our model, $(c_{6H})_{\text{mo}}$, of the polytype SiC-6H, we obtain the following equation

$$(c_{6H})_{\text{mo}} = (c_{4H})_{\text{ex}} + 2(c_{6H})_{\text{ex}}[\tfrac{1}{6} + \delta_{6H}(3) - \delta_{6H}(2)]$$

$$= (c_{4H})_{\text{ex}} + 2\frac{(c_{6H})_{\text{ex}}}{6}\left(1 + \frac{\Delta d_{6H}(2)}{d_0}\right), \tag{12}$$

where $(c_{4H})_{\text{ex}}$ and $(c_{6H})_{\text{ex}}$ are the experimental c lattice constants of the polytypes 4H and 6H (Table 2), respectively, $\Delta d_{6H}(2)/d_0$ is the refinement parameter given in Table 1 (-0.00102 for the model $+1_{6H}$, $+0.00102$ for the model -1_{6H}). The use of the refinement parameter of the carbon atoms instead of the silicon atoms leads to the same results. The

results of this calculation for model $+1_{6H}$ and model -1_{6H} are shown in Table 3.

The relative deviation between the calculated c lattice constant according to (12) and the experimental c lattice constant of the polytype 6H is more than 50 times smaller for model $+1_{6H}$ than for -1_{6H}. Therefore, we conclude that model $+1_{6H}$ describes the polytype 6H. For model $+1_{6H}$, the values of the refinement parameters $\Delta L_{6H}(1, 2)/L_0$ and $\Delta L_{6H}(1, 3)/L_0$ are positive (Table 1). This means that the Si—C bond length in a hexagonal bilayer is larger than in a cubic bilayer. If we assume for the polytype SiC-4H also that the Si—C bond length is larger in a hexagonal bilayer than in a cubic bilayer, the sign of the refinement parameter $\Delta L_{4H}(1, 2)/L_0$ (Table 1) must be positive. Thus, model $+1_{4H}$ describes the structure of the polytype SiC-4H. The influence of the difference in the a lattice constants of the two polytypes is negligible and was therefore not considered.

4. Comparison of *Umweg* scans of 'quasiforbidden' reflections with calculated profiles

Another possibility to distinguish the six structure models of SiC-6H or the two models of SiC-4H is to investigate three-beam cases (*Umweganregung*) of 'quasiforbidden' reflections. The structure factor of a given 'quasiforbidden' reflection of one polytype has the same absolute value for all of our structure models but a different phase. Such phase information can be obtained by a comparison of measured and calculated *Umweg* scans, which allows an unambiguous determination of the refinement parameters without any additional assumptions.

According to (10), the phase difference of our structure refinement models with regard to model $+1_{nH}$ is given by

$$\Delta\varphi_{pq}(hkl) = \frac{\pi l(p-1)}{n/2} + (1-q)\frac{\pi}{2}. \tag{13}$$

In the case of SiC-6H, the phase difference of a given 'quasiforbidden' reflection between each of the six models is $60°$; in the case of SiC-4H, the phase difference between the two models is $180°$.

In three-beam cases (Chang, 1984), there is a superposition of the direct wave, caused by a two-beam diffraction and a second wave, resulting from the *Umweg* diffraction. Phase information can be retrieved from the interference of these two waves. To generate three-beam cases experimentally, the crystal is rotated about the reciprocal-lattice vector **H** (ψ-scan), which is in the reflection position; thereby a second reciprocal-lattice vector **L** is scanned through the Ewald

Table 3
Calculated c lattice constants of the models $+1_{6H}$ and -1_{6H} and the difference between these calculated values and the experimental data.

Model	$(c_{6H})_{mo}$ (Å)	$\|[(c_{6H})_{ex} - (c_{6H})_{mo}]/(c_{6H})_{ex}\|$ (%)
$+1_{6H}$	15.11958	1.2×10^{-3}
-1_{6H}	15.12986	6.7×10^{-2}

sphere. Then automatically a third reflection $\mathbf{H} - \mathbf{L}$ is also in reflection position. The directly diffracted wave and the *Umweg* wave propagate in the same direction. When the reciprocal-lattice vector $\mathbf{L}$ passes through the Ewald sphere, there is a phase shift $\Delta(\psi)$ of the second wave from 0 to $180°$ when the lattice vector $\mathbf{L}$ goes from inside to outside the Ewald sphere (in → out) and from 180 to $0°$ when $\mathbf{L}$ goes from outside to inside (out → in) (Weckert & Hümmer, 1997; Woolfson & Fan, 1995). The total phase difference $\varphi_{tot}(\psi)$ between the primary wave and the *Umweg* wave is

$$\varphi_{tot}(\psi) = \varphi_3 + \Delta(\psi) \quad (14)$$

with

$$\varphi_3 = \varphi_{\mathbf{L}} + \varphi_{\mathbf{H}-\mathbf{L}} - \varphi_{\mathbf{H}}, \quad (15)$$

where φ_3 is the phase invariant of the three-beam case and $\varphi_{\mathbf{H}}$, $\varphi_{\mathbf{L}}$, $\varphi_{\mathbf{H}-\mathbf{L}}$ are the phases of the involved reflections. From this it follows that there is a dependence of the phase-dependent part of the three-beam profiles from $\cos[\varphi_3 + \Delta(\psi)]$ (Hümmer & Weckert, 1995). In our case, $\mathbf{H}$ indicates a weak 'quasiforbidden' reflection ($|F_H| = |F_{qf}| \approx 10^{-1}$), whereas $\mathbf{L}$ and $\mathbf{H} - \mathbf{L}$ are strong reflections ($|F_L|$ and $|F_{H-L}| > 10^1$). Only the structure factor and therewith the phase $\varphi_{\mathbf{H}}$ of the weak reflection $\mathbf{H}$ depends on the refinement parameters. The dependence of the structure factors and their phases of the strong reflections $\mathbf{L}$ and $\mathbf{H} - \mathbf{L}$ from the refinement parameters are negligible, because the deviations from the ideal tetrahedron structure are very small. The strong *Umweg* reflections $\mathbf{L}$ and $\mathbf{H} - \mathbf{L}$ generate a reference wave, which is independent of the refinement parameters. Thus, the difference of the phase invariant φ_3 of the different models depends only on $\varphi_{\mathbf{H}}$ and is therefore $60°$ in the case of SiC-6H and $180°$ in the case of SiC-4H. Since $|F_L|$, $|F_{H-L}| \gg |F_H|$, the phase-independent part owing to *Umweganregung* dominates close to the center of the *Umweg* peaks and phase information can only be obtained from the wings of the *Umweg* peaks, where the amplitudes of the primary and the secondary waves have comparable magnitudes (Chang & Tang, 1988). If the phase invariant φ_3 is close to 0 or $180°$, these wings show a strongly asymmetric behavior. If the distance from the center of the *Umweg* peak is large in comparison to the FWHM of the strong *Umweg* reflection, the additional phase shift $\Delta(\psi)$ is approximately $0°$ $\{\cos[\varphi_3 + \Delta(\psi)] \approx + \cos(\varphi_3)\}$ and $180°$ $\{\cos[\varphi_3 + \Delta(\psi)] \approx - \cos(\varphi_3)\}$, respectively. Since $\cos[\varphi_3 + \Delta(\psi)] \approx \pm \cos(\varphi_3)$, the polarity of the crystal structure has no influence on the wings of the three-beam profiles, *i.e.* $\mathbf{H}$ and $\bar{\mathbf{H}}$ yield the same result. Under this condition, the theory of Shen (1986) is a good approximation to describe the behavior of the wings of the *Umweg* peaks but not of the

center of the peak. This theory is based on the perturbation theory of scattering of electromagnetic waves. It uses a method similar to the second-order Born approximation in quantum mechanics to calculate the integrated intensities of rocking curves of the weak 'quasiforbidden' $000l$ reflections close to three-beam nodes. An exact dynamical calculation was not necessary, because we were only interested in the wings of the *Umweg* peaks and at those positions the extinction is negligible. Furthermore, the requirement to the accuracy are not very high, since the phase differences of the structure factors of 'quasiforbidden' reflections for each model are $180°$ in the case of SiC-4H and $60°$ in the case of SiC-6H.

If $\mathbf{H}$ is a weak 'quasiforbidden' $000l$ reflection, there is in the hexagonal crystal system in addition to the strong reflection $\mathbf{L}$ always another strong reflection $\mathbf{L'}$, which is also located at the Ewald sphere. Therefore also $\mathbf{H} - \mathbf{L'}$ is in the reflection position. The resultant four-beam cases $\mathbf{H}, \mathbf{L'}, \mathbf{L'} - \mathbf{L}, \mathbf{H} - \mathbf{L}$ and $\mathbf{H}, \mathbf{L}, \mathbf{L} - \mathbf{L'}, \mathbf{H} - \mathbf{L'}$, respectively, are negligible because $\mathbf{L'} - \mathbf{L}$ and $\mathbf{L} - \mathbf{L'}$ are always weak 'quasiforbidden' reflections. The two three-beam cases $\mathbf{H}, \mathbf{L}, \mathbf{H} - \mathbf{L}$ and $\mathbf{H}, \mathbf{L'}, \mathbf{H} - \mathbf{L'}$ are equivalent owing to the crystal symmetry, *i.e.* we obtain

$$\frac{F_{\mathbf{H}-\mathbf{L}}F_{\mathbf{L}}}{F_{\mathbf{H}}} = \frac{F_{\mathbf{H}-\mathbf{L'}}F_{\mathbf{L'}}}{F_{\mathbf{H}}} \quad (16)$$

and

$$\varphi_{\mathbf{L}} + \varphi_{\mathbf{H}-\mathbf{L}} - \varphi_{\mathbf{H}} = \varphi_{\mathbf{L'}} + \varphi_{\mathbf{H}-\mathbf{L'}} - \varphi_{\mathbf{H}}. \quad (17)$$

The ψ scans of the 'quasiforbidden' $000l$ reflections for SiC-4H and SiC-6H single-crystal samples were performed at the CRG beamline (ROBL) of the Forschungszentrum Rossendorf at the European Synchrotron Radiation Facility (ESRF) in Grenoble (Matz *et al.*, 1999). The SiC-4H sample was a modified Lely grown crystal (Cree Research) and the
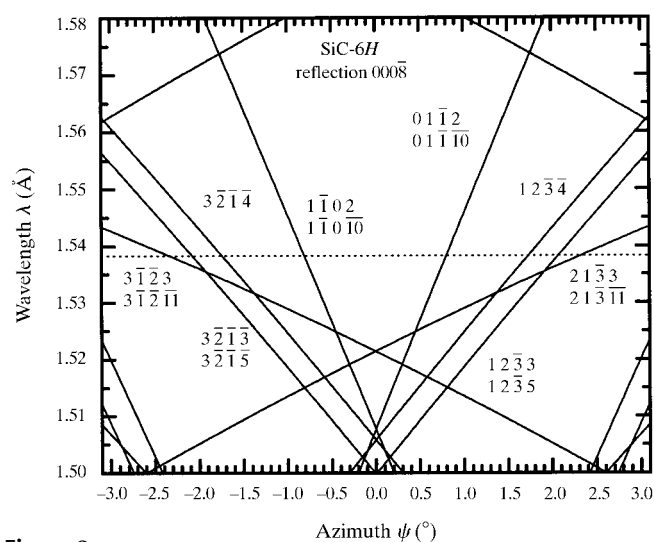

Figure 3
Umweg location plot for the SiC-6H $000\bar{8}$ reflection. The angle 0.0 indicates the [1000] direction in the hexagonal crystal structure. The dotted line indicates the wavelength used. The numbers beside the location lines denote the Miller indices of the strong *Umweg* reflections $\mathbf{L}$ and $\mathbf{L'}$ (*cf.* Fig. 5).

Table 4
Phase invariants φ_3 of the six different SiC-6H models of the Umweg reflections **L** and **L**′ (cf. Fig. 4) of the 'quasiforbidden' $000\bar{2}$ reflection in °.

out → in means that the azimuthal scan is carried out so that **L** and **L**′ pass the Ewald sphere from outside to inside.

L/L′	$+1_{6H}$	-1_{6H}	$+2_{6H}$	-2_{6H}	$+3_{6H}$	-3_{6H}
$12\bar{3}\bar{1}/12\bar{3}\bar{1}$ (out → in)	−172	8	−52	128	68	−112
$12\bar{3}1/12\bar{3}\bar{3}$ (out → in)	−6	174	114	−66	126	54
$12\bar{3}2/12\bar{3}\bar{4}$ (out → in)	154	−26	−86	94	34	−146
$1\bar{1}03/1\bar{1}0\bar{5}$ (in → out)	−47	133	73	−107	−167	13

Table 5
Phase invariants φ_3 of the SiC-6H models $+1_{6H}$ and -3_{6H} of the Umweg reflections **L** and **L**′ of the 'quasiforbidden' $000\bar{8}$ reflection in °.

L/L′	$+1_{6H}$	-3_{6H}
$01\bar{1}2/01\bar{1}\bar{1}0$ (out → in)	−148	−88
$12\bar{3}4/12\bar{3}\bar{4}$ (out → in)	−140	−80
$12\bar{3}\bar{3}/12\bar{3}\bar{5}$ (out → in)	40	100
$21\bar{3}3/21\bar{3}\bar{1}1$ (out → in)	41	101

is opposite, since the reciprocal-lattice vector **L** goes from the inside to the outside through the Ewald sphere (in → out) or vice versa (out → in), e.g. the $1\bar{1}02$ and $01\bar{1}2$ reflections in Fig. 3.

A comparison of measured and calculated ψ-scan profiles for the SiC-6H reflection $000\bar{2}$ is shown in Fig. 4. Fig. 4(a) shows the measured ψ-scan profile of the 'quasiforbidden' reflection $000\bar{2}$ and Figs. 4(b)–(d) the calculated profiles of the

SiC-6H sample a Lely platelet. Both samples were cut on an axis perpendicular to the [0001] direction. The surface of the SiC-4H crystal was silicon terminated [(0001) plane], while the surface of the SiC-6H crystal was carbon terminated [$(000\bar{1})$ plane]. The area of the sample surface was a couple of square centimeters. The thickness of the samples was about 0.5 mm. The X-ray beam was produced by a bending magnet, collimated at a silicon mirror, passed through a double-crystal silicon monochromator of fixed exit type with Si (111) and a focusing second silicon mirror. The two-mirror arrangement suppresses higher harmonics better than 10^{-4}. The wavelengths used were 1.5383 and 1.5440 Å. For investigation of the samples, a six-circle goniometer with x–y–z table (Huber) was at our disposal. The beam cross section was 0.3×0.3 mm. The X-ray beam was π polarized.

A direct comparison of the measured ψ-scans with the calculated integrated intensities according the theory of Shen is possible because the contribution from the instrument (FWHM approximately 0.003°) is much broader than the intrinsic rocking curve (FWHM approximately $10^{-4\circ}$) and the sample crystals were almost perfect. This means that the FWHM of a rocking curve of a 'quasiforbidden' reflection is only determined by the apparatus function. Then the integrated intensity of the 'quasiforbidden' $000l$ reflections is proportional to the maximum intensity of a rocking curve, which is measured at a ψ scan. For the calculations of the ψ-scans we used the refinement parameter given in Table 1.

In the case of a $000l$ reflection **H**, the ψ position of an Umweg reflection **L** can be calculated using, similar to Cole et al. (1962), the following equation:

$$\lambda = \frac{2d_{\mathbf{H}} \cos \psi}{[\cos^2 \psi + (d_{\mathbf{L}} \cot \alpha - d_{\mathbf{H}} \mathrm{cosec}\, \alpha)^2 / d_{\mathbf{L}}^2]^{1/2}}, \quad (18)$$

where λ is the wavelength, α is the angle between the reciprocal-lattice vector **H** and **L**, $d_{\mathbf{H}}$, $d_{\mathbf{L}}$ are the lattice plane distances of these reflections, and ψ is the azimuthal angle relating to the [1000] direction. According to point group $6mm$, 12 equivalent Umweg reflections would appear in a 360° azimuthal ψ scan. Arbitrarily, the (1000) mirror plane was chosen as the azimuthal zero point. Fig. 3 shows according to (18) the azimuthal angles of all possible three-beam reflections at a selected wavelength range for the 'quasiforbidden' SiC-6H $000\bar{8}$ reflection. Positions of equivalent Umweg reflections are located azimuthally symmetric to the zero position, whereby the asymmetric pattern of the Umweg peaks

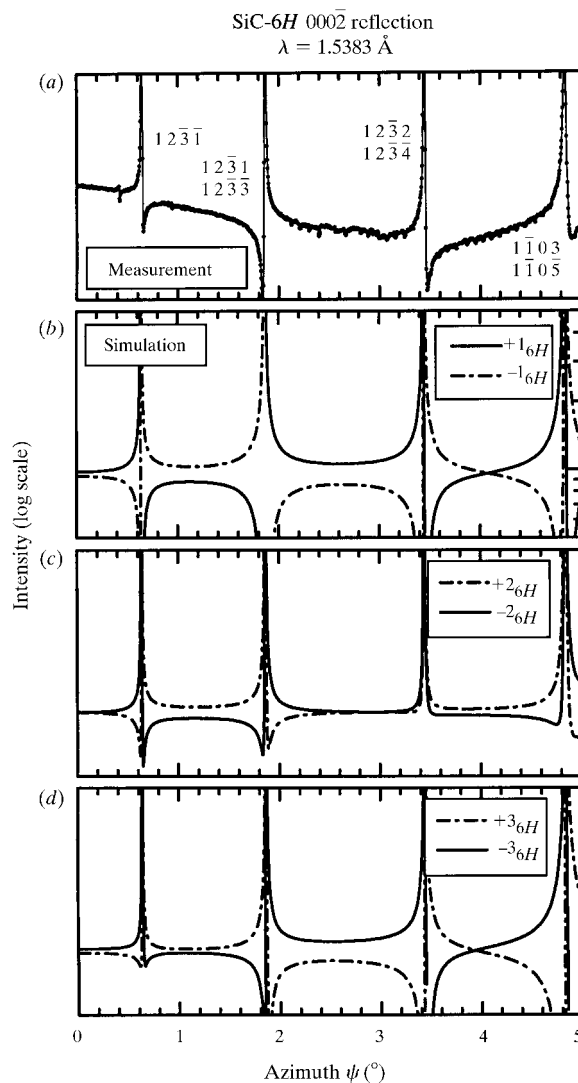SiC-6H $000\bar{2}$ reflection
$\lambda = 1.5383$ Å

Figure 4
(a) Measured azimuth scan of the SiC-6H $000\bar{2}$ reflection. The numbers beside the Umweg peaks denote the Miller indices of the strong reflections **L** and **L**′. (b)–(d) Calculated azimuth scans of the six different models of the same reflection.

six models. Only the two models $+1_{6H}$ and -3_{6H} match qualitatively with the measured ψ-scan. Unfortunately, the two models show very similar ψ-scan profiles because the $\cos(\varphi_3)$ of these two models of each of the four displayed *Umweg* reflections has the same algebraic sign. The calculated phase invariants of the 'quasiforbidden' $000\bar{2}$ reflection are shown in Table 4. The asymmetry of the wings of the *Umweg* peaks is according to the approximation of Shen, besides some geometric factors, related to the cosine of the invariant phase φ_3. A change of the sign of the cosine of φ_3 leads to an opposite asymmetric pattern of the *Umweg* peak. However, this theory results in the same *Umweg* profiles for the phase invariants φ_3 and $-\varphi_3$ because $\cos(\varphi_3)$ and $\cos(-\varphi_3)$ are identical. Additionally, Fig. 4 also shows a decreasing two-beam intensity of the weak $000\bar{2}$ reflection in the direction of positive angles. This is caused by a small maladjustment of the sample, which means that the lattice-plane normal was not exactly parallel to the rotation axis.
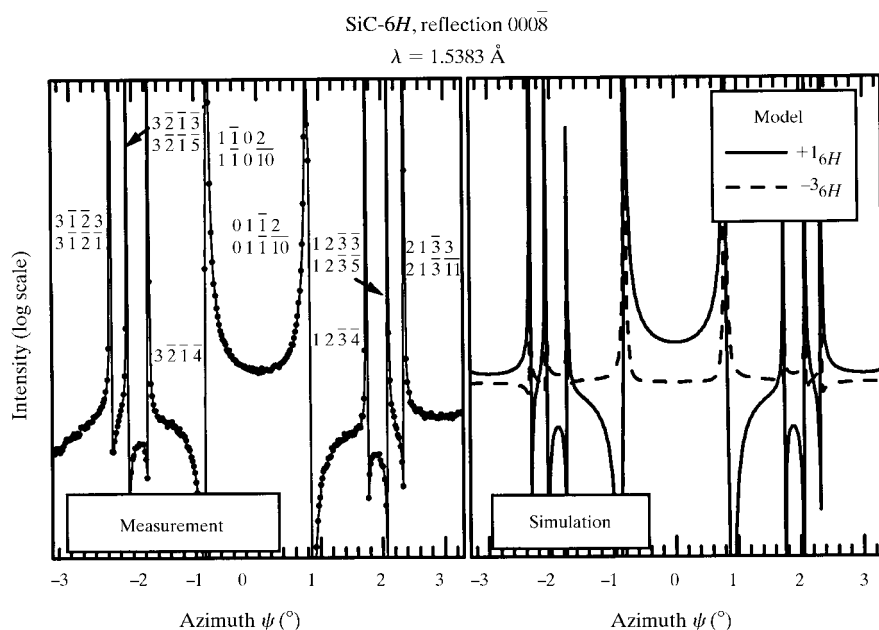
In order to distinguish the two models $+1_{6H}$ and -3_{6H}, another ψ scan was performed on the 'quasiforbidden' $000\bar{8}$ reflection of SiC-6H (Fig. 5). The phase invariants of this reflection are given in Table 5. Now it can be seen clearly that only the model $+1_{6H}$ is in accordance with the measured ψ-scan profile.

For the polytype SiC-4H, an unambiguous distinction of the two models is easier because the difference of the phase invariant φ_3 for models $+1_{4H}$ and -1_{4H} is $180°$. The asymmetric wings of the three-beam peaks possess the opposite behavior for models $+1_{4H}$ and -1_{4H}. Fig. 6 shows a comparison of a measured ψ-scan of the 'quasiforbidden' SiC-4H reflection 0002 with the calculated curves of models $+1_{4H}$ and -1_{4H} and Table 6 shows the corresponding phase invariants. Only model $+1_{4H}$ matches the measured ψ-scan profile.

For both SiC-6H and SiC-4H, model $+1_{nH}$ is in accordance with the structure refinement parameters, which were found by *ab initio* calculations from Käckell *et al.* (1994) and Cheng *et al.* (1990).

Figure 5
Left: measured azimuth scan of the SiC-6H $000\bar{8}$ reflection. The numbers beside the *Umweg* peaks denote the Miller indices of the strong reflections **L** and **L**'. Right: calculated azimuth scans of the two remaining models $(+1_{6H}, -3_{6H})$ of the same reflection.
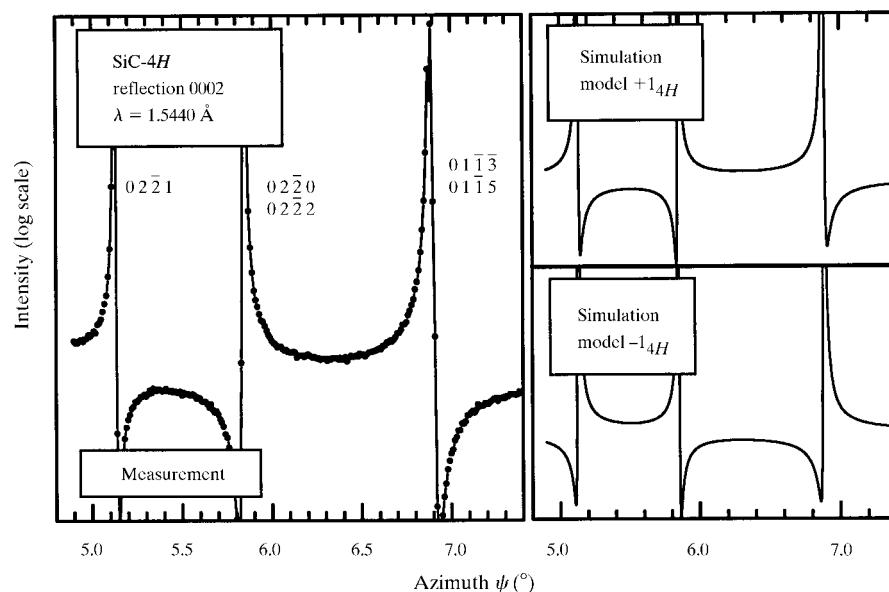

Figure 6
Left: experimental azimuth scan of the SiC-4H 0002 reflection. The numbers beside the *Umweg* peaks denote the Miller indices of the strong reflections **L** and **L**'. Top right: simulation of the SiC-4H 0002 reflection model $+1_{4H}$. Bottom right: simulation of the SiC-4H 0002 reflection model -1_{4H}.

5. Summary

The use of 'quasiforbidden' reflections allows high-precision determination of relaxation parameters of SiC-4H and SiC-6H, but this method is ambiguous. We have proposed two approaches to get an unambiguous determination of the relaxation parameters of these silicon carbide polytypes. By means of a comparison of the internal structure of the unit cells and the precisely measured lattice constants of SiC-4H and SiC-6H, it was possible to abolish the ambiguity in respect of the six different structure models of SiC-6H as well as the two models of SiC-4H. This method works only with the assumption of the equivalence of both cubic bilayers of the

Table 6
Phase invariants φ_3 of the SiC-4H models $+1_{4H}$ and -1_{4H} of the *Umweg* reflections **L** and $\mathbf{L}'$ of the 'quasiforbidden' 0002 reflection in °.

$\mathbf{L}/\mathbf{L}'$	$+1_{6H}$	-3_{6H}
$02\bar{2}1/02\bar{2}1$ (out → in)	−155	25
$02\bar{2}0/02\bar{2}2$ (out → in)	13	−167
$01\bar{1}3/01\bar{1}5$ (out → in)	−175	5

polytype SiC-6H. Without any additional assumptions, it was possible to distinguish the six different models of SiC-6H as well as the two models of the polytype 4H by a comparison of measured ψ-scan profiles of 'quasiforbidden' reflections close to three-beam nodes with calculated profiles according to a second-order Born approximation of Shen, because the phase differences of the structure factors of 'quasiforbidden' reflections for each model are discrete and equidistant. Using this method, neither an exact adjustment of the calculated profiles to the measured data nor a dynamical calculation was necessary to reach this aim. Both methods to obtain an unambiguous structure refinement model led to the same result, which is also in agreement with theoretical models obtained by *ab initio* calculations.

References

Bauer, A., Kräusslich, J., Dressler, L., Kuschnerus, P., Wolf, J., Goetz, K., Käckell, P., Furthmüller, J. & Bechstedt F. (1998). *Phys. Rev. B*, **57**, 2647–2650.

Bauer, A., Kräusslich, J., Kuschnerus, P., Goetz, K., Käckell, P. & Bechstedt, F. (1999). *Mater. Sci. Eng. B*, **61-62l**, 217–220.

Chang, S. L. (1984). *Multiple Diffraction of X-rays in Crystals.* Berlin/Heidelberg/New York: Springer Verlag.

Chang, S. L. & Tang, M. T. (1988). *Acta Cryst.* A**44**, 1065–1072.

Cheng, C., Heine, V. & Needs, R. J. (1990). *J. Phys. Condens. Matter*, **2**, 5115–5134.

Cole, H., Chambers, F. W. & Dunn, H. M. (1962). *Acta Cryst.* **15**, 138–144.

Harris G. L. (1995). *Properties of Silicon Carbide.* London: INSPEC.

Hümmer, K. & Weckert, E. (1995). *Acta Cryst.* A**51**, 431–438.

Käckell, P., Wenzien, B. & Bechstedt, F. (1994). *Phys. Rev. B*, **50**, 17037–17046.

Matz, W., Schell, N., Bernhard, G., Prokert, F., Reich, T., Claussner, J., Oehme, W., Schlenk R., Dienel, S., Funke, H., Eichhorn, F., Betzl, M., Pröhl, D., Strauch, U., Hüttig, G., Krug, H., Neumann, W., Brendler, V., Reichel, P., Deneke, M. A. & Nitsche, H. (1999). *J. Synchrotron Rad.* **6**, 1076–1085.

Shen, Q. (1986). *Acta Cryst.* A**42**, 525–533.

Starke, U. (1997). *Phys. Status Solidi B*, **202**, 475–499.

Verma, A. R. & Krishna, P. (1966). *Polymorphism and Polytypism in Crystals.* New York: Wiley.

Weckert, E. & Hümmer, K. (1997). *Acta Cryst.* A**53**, 108–143.

Woolfson, M. M. & Fan, H.-F. (1995). *Physical and Non-Physical Methods of Solving Crystal Structures.* Cambridge University Press.